A peripheral CD4+ T cell precursor for naive, memory, and regulatory T cells

Chunfang Zhao and Joanna D. Davies

Torrey Pines Institute for Molecular Studies, 3550 General Atomics Court, San Diego, CA 92121

Mechanisms that control the size of the T cell pool, the ratio between naive cells and memory cells, the number and frequency of regulatory T cells, and T cell receptor (TCR) diversity are necessary to maintain immune integrity and avoid disease. We have previously shown that a subset of naive CD4+ T cells, defined by the expression on their surface of a very low density of CD44 (CD44v.low cells), can inhibit wasting and wasting-associated lymphopenia in mice with cancer. In this study, we further investigate the properties of CD44v.low cells and show that they are significantly more efficient than the remaining naive (CD44low or CD44int) and memory CD4+ cell subsets in reconstituting the overall size of the CD4+ T cell pool, creating a T cell pool with a diverse TCR repertoire, generating regulatory T cells that express forkhead box P3 (FoxP3), and promoting homeostatic equilibrium between naive, memory, and Foxp3+ regulatory T cell numbers. T cell population reconstitution by CD44v.low cells is thymus independent. Compared with CD44int cells, a higher percentage of CD44v.low cells express B cell leukemia/lymphoma 2, interleukin-7 receptor, and CD5. The data support a key role for CD4+ CD44v.low cells as peripheral precursors that maintain the integrity of the CD4+ T cell pool.

CORRESPONDENCE
Joanna D. Davies:
jdavies@tpims.org

Abbreviation used: ANOVA, analysis of variance; APC, allophycocyanin; aTreg, acquired Treg; Bcl-2, B cell leukemia/lymphoma 2; CDR3, complementary determining region 3; Foxp3, forkhead box P3; nTreg, natural Treg; SCID, severe combined immunodeficiency; Treg, regulatory T cell.

In a fully functional immune system, the size and diversity of the CD4+ T cell pool is maintained at a constant level by homeostatic mechanisms (Freitas and Rocha, 1993; Bell and Sparshott, 1997; Min et al., 2005). Immune cell insufficiency and dysregulation of CD4+ T cell homeostasis is associated with a variety of primary disease conditions. These include autoimmunity (Jonsson et al., 2002), chronic infection (McMichael and Rowland-Jones, 2001), and cancer (Miller et al., 1997), conditions that can lead to cachexia, the dramatic wasting syndrome seen in many chronic diseases (Lainscak et al., 2008). Previously, we showed that cachexia and cachexia-associated lymphopenia was inhibited by the infusion of CD4+ CD44v.low cells into mice with cancer (Wang et al., 2008).

CD4+ CD44v.low cells are operationally defined as those cells with the lowest CD44 expression. The cell surface expression of CD44 is used to phenotypically distinguish naive from memory CD4+ T cells. Thus, naive cells express a low level of CD44 (CD44low), whereas memory cells express a high level (CD44high; Budd et al., 1987; Swain, 1994). CD4+ CD44v.low cells constitute the 2–5% of the total naive CD4+ CD44low cell population that expresses the lowest density of CD44. They also express a high density of both CD45RB and CD62L (Zhao et al., 2008), which also define them as being naive (Bottomly et al., 1989; Lee et al., 1990; Swain, 1994). The naive CD4+ CD44low cells that are not CD4+ CD44v.low cells have been termed CD44 intermediate (CD44int; Wang et al., 2008). Thus, naive CD4+ CD44low cells consists of two populations, CD4+ CD44v.low cells and CD4+ CD44int cells. CD4+ CD44v.low cells were first identified by the observation that CD4+ cells expressing a very low density of CD44 are absent from the spleens and lymph nodes of cachexic mice (Zhao et al., 2008). In contrast, neither CD4+ CD44int nor CD4+ CD44high cells are absent from these mice (Zhao et al., 2008). Moreover, unlike CD4+ CD44v.low cells, CD4+ CD44int and CD4+ CD44high cells do not inhibit cachexia and cachexia-associated lymphopenia, indicating a novel function for CD4+ CD44v.low cells (Wang et al., 2008).

The Rockefeller University Press $30.00
J. Exp. Med. Vol. 207 No. 13 2883-2894
www.jem.org/cgi/doi/10.1084/jem.20100598

The Journal of Experimental Medicine

In this study, we further describe the properties of this novel $CD4^+$ T cell subset and show that it has a unique ability to maintain the integrity of the $CD4^+$ T cell population by expanding and differentiating into naive, memory, and forkhead box P3 (Foxp3)$^+$ regulatory $CD4^+$ T cell subsets having a diverse TCR repertoire. Collectively, the data support a key role for $CD4^+$ $CD44^{v.low}$ cell function as part of the homeostatic mechanism to maintain the size and diversity of the $CD4^+$ T cell pool. These findings indicate that enhancing $CD4^+$ $CD44^{v.low}$ cell numbers or their function may provide a therapeutic approach for disease- and drug-induced lymphopenia and lymphopenia-associated disease.

RESULTS

$CD4^+$ $CD44^{v.low}$ cells are significantly more effective than other naive $CD4^+$ cells in their ability to expand and accumulate in lymphopenic hosts

To test the capacity of $CD4^+$ $CD44^+$ cells to repopulate peripheral T cells in lymphopenic hosts, groups of CB17. Severe combined immunodeficiency (SCID) mice were injected with $CD4^+$ $CD44^{v.low}$ cells, with $CD44^{v.low}$-depleted $CD4^+$ cells (i.e., that contained $CD44^{int}$ and $CD44^{high}$ cells), or with no cells. The number of $CD4^+$ T cells in the spleens of recipient mice at 9 and 13 wk after cell infusion was then determined by FACS analysis. Mice that were injected with $CD4^+$ $CD44^{v.low}$ cells contained significantly more $CD4^+$ T cells than did mice that received $CD44^{v.low}$-depleted $CD4^+$ cells (Fig. 1 A). This was also observed in lymph nodes (unpublished data). Notably, the levels of $CD4^+$ reconstitution at 3, 9, and 13 wk were very similar. Therefore, mice were analyzed at 3 wk after cell transfer in all subsequent experiments.

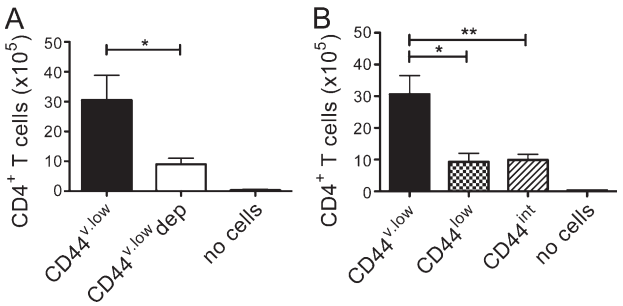

Figure 1. $CD4^+$ $CD44^{v.low}$ cells are significantly more effective in their ability to expand and accumulate in lymphopenic hosts than other naive $CD4^+$ cells. (A) CB17.SCID mice were injected with 2.5×10^5 purified $CD4^+$ $CD44^{v.low}$ cells ($n = 4$), with an equal number of purified $CD4^+$ cells depleted of $CD44^{v.low}$ cells ($CD44^{v.low}$ dep; $n = 4$), or with no cells ($n = 4$). Mice were sacrificed at 9 ($n = 2$ per group) or 13 ($n = 2$ per group) wk after cell transfer, and the number of $CD4^+$ T cells in the spleens was determined by FACS. Data were pooled for each group at the two time points. (B) CB17.SCID mice were injected with 2.5×10^5 purified $CD4^+$ $CD44^{v.low}$ cells ($n = 6$), with $CD4^+$ $CD44^{int}$ cells ($n = 6$), with $CD4^+$ $CD44^{low}$ cells ($n = 5$), or with no cells ($n = 2$). Mice were sacrificed 3 wk after cell transfer, and the number of $CD4^+$ T cells in the spleens was determined by FACS. Data are shown as mean ± SEM and are representative of two independent experiments. One-way ANOVA shows a significance of P = 0.005 for A and P = 0.001 for B. Significance between groups using Bonferroni's multiple comparison test is indicated on the figures.
*, P = 0.01–0.05; **, P = 0.001–0.01.

In these experiments, it was possible that $CD4^+$ $CD44^{high}$ cells present within the $CD44^{v.low}$-depleted $CD4^+$ cells may have suppressed the capacity of $CD4^+$ $CD44^{int}$ cells to expand and accumulate. To exclude this possibility we compared the ability of $CD4^+$ $CD44^{v.low}$, or $CD4^+$ $CD44^{int}$, or $CD4^+$ $CD44^{low}$ (containing $CD4^+$ $CD44^{v.low}$ and $CD4^+$ $CD44^{int}$) cells to reconstitute SCID mouse recipients. As shown in Fig. 1 B, the size of the $CD4^+$ T cell population derived from $CD4^+$ $CD44^{v.low}$ cells was significantly greater than that derived from either $CD4^+$ $CD44^{low}$ cells or $CD4^+$ $CD44^{int}$ cells. These data are consistent with the hypothesis that $CD4^+$ $CD44^{v.low}$ cells are superior to $CD4^+$ $CD44^{int}$ cells in their capacity to expand in lymphopenic hosts, and that the two are functionally distinct populations within the $CD4^+$ $CD44^{low}$ naive cells.

$CD4^+$ $CD44^{v.low}$ cells generate naive and memory phenotype cells at a ratio that suggests homeostatic equilibrium

Under normal circumstances, the ratio of naive and memory T cells in the periphery is highly regulated. To determine if $CD4^+$ $CD44^{v.low}$ cells retain a normal ratio of naive and memory cells, CB17.SCID mice were infused with $CD4^+$ $CD44^{v.low}$ cells, $CD4^+$ $CD44^{int}$ cells, $CD4^+$ $CD44^{high}$ cells, or with no cells, and the number and ratio of $CD4^+$ T cell subsets was determined 3 wk later. $CD4^+$ $CD44^{int}$ cells and $CD44^{high}$ cells were shown to be equivalent in their ability to expand and accumulate $CD4^+$ T cells, but both were significantly less efficient than $CD4^+$ $CD44^{v.low}$ cells (Fig. 2 A). In addition, $CD4^+$ $CD44^{v.low}$ cells are significantly more effective in producing populations of $CD4^+$ $CD44^{int}$ (Fig. 2 B) and $CD4^+$ $CD44^{high}$ (Fig. 2 C) cells than those that were infused $CD4^+$ $CD44^{int}$ and $CD4^+$ $CD44^{high}$ cells themselves. Moreover, whereas splenocytes from mice infused with $CD4^+$ $CD44^{v.low}$ cells contained substantial numbers of $CD4^+$ $CD44^{v.low}$ cells, $CD4^+$ $CD44^{int}$ cells were very inefficient at producing these cells (Fig. 2 D).

The ratio of cells with a naive phenotype ($CD4^+$ $CD44^{v.low}$ and $CD44^{int}$ cells) and a memory phenotype ($CD44^{high}$ cells) in mice reconstituted with $CD4^+$ $CD44^{v.low}$ cells was very similar to that in untreated BALB/c mice (Fig. 2 E). Thus, the $CD4^+$ $CD44^{v.low}$ cells more efficiently expand a cell population with a naive phenotype than do $CD4^+$ $CD44^{int}$ cells. In contrast, the $CD4^+$ $CD44^{int}$ cells and $CD4^+$ $CD44^{high}$ cells are more efficient in expanding the memory cell pool than the $CD4^+$ $CD44^{v.low}$ cell population (Fig. 2 E). Thus, the expanded cell population derived from $CD4^+$ $CD44^{v.low}$ cells retained a ratio of naive/memory cells that was similar to that in untreated wild-type animals.

$CD4^+$ $CD44^{v.low}$ cells generate Foxp3$^+$ regulatory cells more efficiently than do $CD4^+$ $CD44^{int}$ cells

A functionally balanced immune system depends on the presence of regulatory cells, including those that express Foxp3 (regulatory T cells [Tregs]). Foxp3-expressing cells are either

rare or absent in purified CD4+ CD44v.low cells, but are readily detectable in CD4+ CD44int cells (Fig. S1 and Table S1). Thus, to determine the relative ability of CD4+ CD44v.low and CD4+ CD44int cells to reconstitute Foxp3+ Tregs, we depleted Foxp3-expressing cells from CD4+ CD44int population by cell sorting. For these experiments, the source of each purified cell population was the Foxp3-GFP mouse strain, in which all Foxp3-expressing cells coexpress GFP. Sorted Foxp3− cells of either the CD4+ CD44v.low or the CD4+ CD44int subset were then transferred into SCID mice, and the expression of Foxp3 in spleen CD4+ T cells was determined 3 wk later.

In animals infused with CD4+ CD44v.low cells, between 10 and 20% of CD4+ T cells expressed Foxp3 (Fig. 3 A). Although mice that received Foxp3-depleted CD4+ CD44int cells did generate CD4+ Foxp3+ cells, their reconstitution was much more inefficient with respect to both percentage (Fig. 3 A) and total number (Fig. 3 B) of Foxp3+ cells when compared with mice that received CD4+ CD44v.low cells.

Reconstitution of CD4+ naive and regulatory cells by CD44v.low cells does not require thymopoiesis

The mechanism of naive cell reconstitution in lymphopenic hosts has been studied extensively, and the conclusion thus far is that naive cells can only be generated by thymopoiesis (Ge et al., 2002). Our data challenge this paradigm by suggesting that naive cells can be generated in the periphery from CD4+ CD44v.low precursor cells (Fig. 2 B). The generation of Foxp3+ cells from naive cell inoculation into lymphopenic hosts has also not been previously described, and our data suggest that naive CD4+ CD44int cells are not efficient in this respect (Fig. 3). To exclude the possibility that the CD4+ CD44v.low cells, or a subset of cells within the CD4+ CD44v.low cell population migrate to the thymus and develop into cells that then seed the peripheral immune system, we tested the ability of CD4+ CD44v.low cells to reconstitute naive, memory, and Foxp3+ regulatory cells in thymectomized CB17.SCID mice. CD4+ CD44v.low cells reconstituted total CD4 (Fig. 4 A), Foxp3+ (Fig. 4 B), CD44v.low (Fig. 4 C), CD44int (Fig. 4 D), and CD44high (Fig. 4 E) cells equally well in thymectomized and euthymic CB17.SCID mice. Reconstitution of cell subsets by CD44int cells is shown as a comparison to emphasize efficient reconstitution by CD44v.low cells (Fig. 4, A–E).

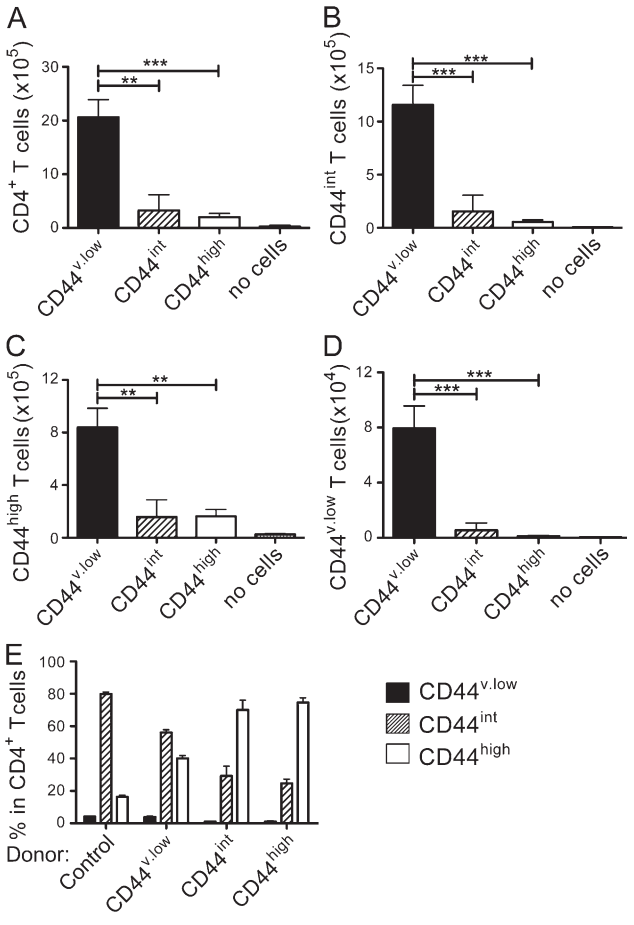

Figure 2. CD4+ CD44v.low cells generate naive and memory phenotype cells at a ratio that suggests homeostatic equilibrium. CB17.SCID mice were injected with 2.5 × 10^5 purified CD4+ CD44v.low cells (n = 5), purified CD4+ CD44int cells (n = 4), purified CD4+ memory (CD44high) cells (n = 4), or no cells (n = 4). Mice were sacrificed 3 wk after cell transfer, and the number of total CD4+ T cells (A), CD4+ CD44int cells (B), CD4+ CD44high cells (C), and CD4+ CD44v.low cells (D) in the spleens was determined by FACS. (E) The percentage of CD4+ T cells that express CD44v.low (black bars), CD44int (hatched bars), or CD44high (white bars) phenotypes in spleens of untreated BALB/c mice (control) and in SCID mice reconstituted with CD4+ CD44v.low, CD4+ CD44int, or CD4+ CD44high cells. Data are shown as mean ± SEM, are pooled from two separate experiments, and are representative of three independent experiments. One-way ANOVA showed significance of P < 0001, P < 0.001, P = 0.004, and P = 0.001 for A, B, C, and D, respectively. Significance between groups using Bonferroni's multiple comparison test is indicated on the figures. **, P = 0.001–0.01; ***, P < 0.001.

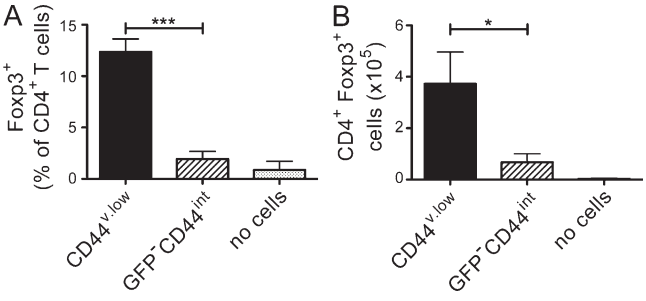

Figure 3. CD4+ CD44v.low cells reconstitute Foxp3+ cells more efficiently than CD4+ CD44int cells. CB17.SCID recipients were injected with 2.5 × 10^5 CD4+ CD44v.low cells (n = 8) or an equal number of CD4+ CD44int cells sorted from GFP− CD4+ splenocytes (n = 10) from Foxp3-GFP transgenic mice, or with no cells (n = 8). 3 wk later, the percentage (A) and the total number (B) of CD4+ Foxp3+ cells were determined by FACS. The experiment was performed twice, and the data presented are pooled from the two independent experiments and shown as mean ± SEM. One-way ANOVA showed significance of P < 0001 and P = 0.007 for A and B, respectively. Significance between groups using Bonferroni's multiple comparison test is indicated on the figures. *, P = 0.01–0.05; *** P < 0.001.

Because CD44^{int} cells contain Foxp3$^+$ cells it is likely that a significant proportion of the Foxp3$^+$ cells in this group are Foxp3$^+$ Tregs present in the initial cell inoculum and not newly converted Foxp3$^+$ Tregs.

Previously published studies show that naive T cells can circulate back to the thymus in SCID and Rag-deficient recipient mice (Surh et al., 1992; Kirberg et al., 2008). To determine whether CD44$^{v.low}$ cells have a similar capacity, euthymic mice were infused with either CD44$^{v.low}$ or CD44^{int} cells, and the number of CD3$^+$ cells was determined 3 wk later. CD44$^{v.low}$- (Fig. 4 F) and CD44^{int}-derived (Fig. 4 G) cells circulate to the thymus with similar capacity, with 0.52 ± 0.19% and 0.66 ± 0.12% thymus cells in mice infused with either CD44$^{v.low}$ or CD44^{int} cells expressing CD3, respectively. Moreover, the CD3$^+$ cells in thymi of both groups were CD4$^+$ CD8$^-$ single-positive, suggesting that neither CD44$^{v.low}$ nor CD44^{int} cells colonize the thymus with immature thymocytes for later export into the periphery (Fig. 4 F and Fig. 4 G).

Intravenous injection of CD44$^{v.low}$ cells also results in reconstitution of naive and regulatory CD4$^+$ cells

The route of T cell inoculation can result in both qualitative and quantitative differences in immune cell function. To determine whether the capacity of CD4$^+$ CD44$^{v.low}$ cells to reconstitute naive and regulatory cell subsets is restricted to inoculation by the peritoneal route, we directly compared reconstitution of both CD4$^+$ CD44$^{v.low}$ and CD4$^+$ CD44^{int} cells by peritoneal and intravenous injection. Reconstitution by both cell subsets is more efficient when infused intravenously compared with peritoneal injection. However, consistent with data shown in Figs. 1–4, reconstitution of total CD4 (Fig. 5 A), CD44$^{v.low}$ (Fig. 5 B), CD44^{int} (Fig. 5 C), CD44^{high} (Fig. 5 D), and Foxp3$^+$ (Fig. 5 E) cell subsets is significantly more efficient in mice given CD4$^+$ CD44$^{v.low}$ cells than in mice given CD4$^+$ CD44^{int} cells when infused via the intravenous route, indicating that efficient reconstitution of naive and regulatory cells by CD4$^+$ CD44$^{v.low}$ cells is not restricted to reconstitution via the peritoneal route.

The CD4$^+$ CD44$^{v.low}$ cells are functionally naive

To determine whether CD4$^+$ CD44$^{v.low}$ cells have the functional characteristics of naive CD4$^+$ T cells consistent with their naive phenotype (Zhao et al., 2008), we tested their ability to proliferate in response to anti-CD3 mAb, and their dependency on co-stimulation, compared with the naive CD4$^+$ CD44^{int} cells. CD4$^+$ Foxp3$^+$ cells are known to influence T cell proliferation, and because Foxp3$^+$ cells are not equally distributed within the CD4$^+$ cell subsets to be tested, Foxp3$^-$ cell subsets were sorted from Foxp3-GFP mice to yield highly purified CD4$^+$ CD44$^{v.low}$ Foxp3$^-$ cells, CD4$^+$ CD44^{int} Foxp3$^-$ cells, and CD4$^+$ CD44^{high} Foxp3$^-$ cells. The cells were cultured with plate-bound anti-CD3, in the presence and absence of anti-CD28 mAb co-stimulation. Proliferation was measured daily from day 2–5 of culture. As expected, we found that proliferation of memory CD4$^+$ T cells was significantly greater than proliferation of naive CD4$^+$ CD44^{int} cells to anti-CD3 alone (Fig. 6 A). Proliferation by memory CD4$^+$ CD44^{high} and CD4$^+$ CD44^{int} cells was also significantly greater than proliferation by CD4$^+$ CD44$^{v.low}$ cells under the same culture conditions (Fig. 6 A). However, CD4$^+$ CD44$^{v.low}$ cells proliferated more vigorously than CD4$^+$ CD44^{int} cells in the presence of anti-CD28 (Fig. 6 B), suggesting that they possess greater sensitivity to co-stimulation.

We next measured IL-2 levels on days 3 and 4 of culture, and found significantly lower levels in the supernatants harvested from CD4$^+$ CD44$^{v.low}$ cells compared with those from CD4$^+$ CD44^{int} cells (Fig. 6 C).

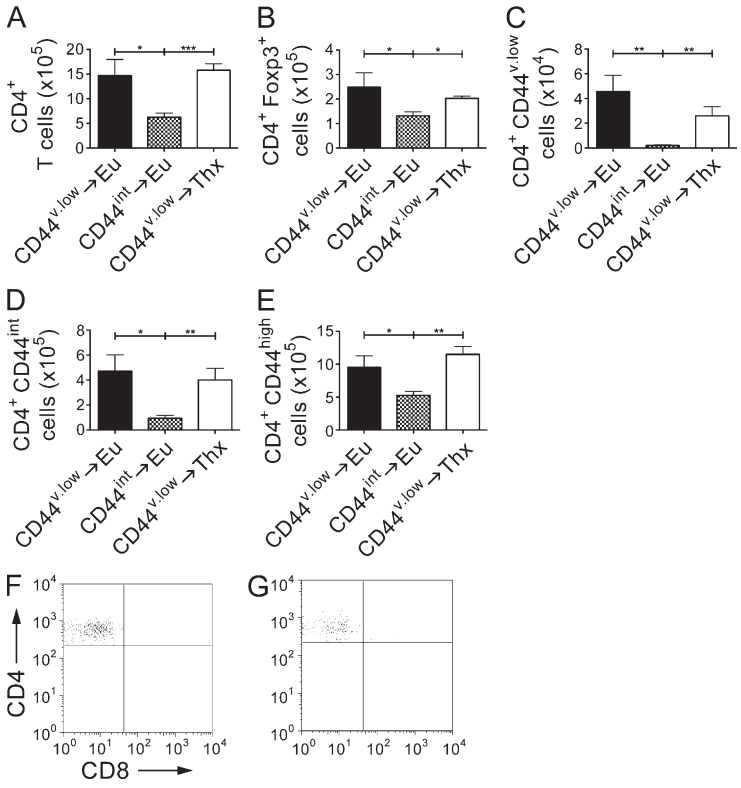

Figure 4. Reconstitution of CD4$^+$ naive and regulatory cells by CD44$^{v.low}$ cells does not require thymopoiesis. Euthymic (Eu, $n = 6$) and thymectomized (Thx, $n = 3$) CB17.SCID mice were reconstituted with 2.5×10^5 purified CD4$^+$ CD44$^{v.low}$ cells. An additional group of euthymic CB17.SCID mice was infused with 2.5×10^5 purified CD4$^+$ CD44^{int} cells ($n = 6$). 3 wk later, the total number of CD4$^+$ (A), Foxp3$^+$ (B), CD44$^{v.low}$ (C), CD44^{int} (D), and CD44^{high} (E) cells in the spleens of thymectomized and euthymic mice was determined by FACS. At the same time, the thymi were removed from all euthymic CD44$^{v.low}$ (F) and CD44^{int} (G) recipient mice. Single-cell suspensions were co-stained with antibodies specific for CD3, CD4, and CD8 and analyzed by FACS. Dot plots are gated on CD3$^+$ cells and are representative of all samples in two experiments. Data are shown as mean ± SEM and are representative of two experiments. Significance between groups is indicated on the panels. *, P = 0.01–0.05; **, P = 0.001–0.01; and ***, P < 0.001.

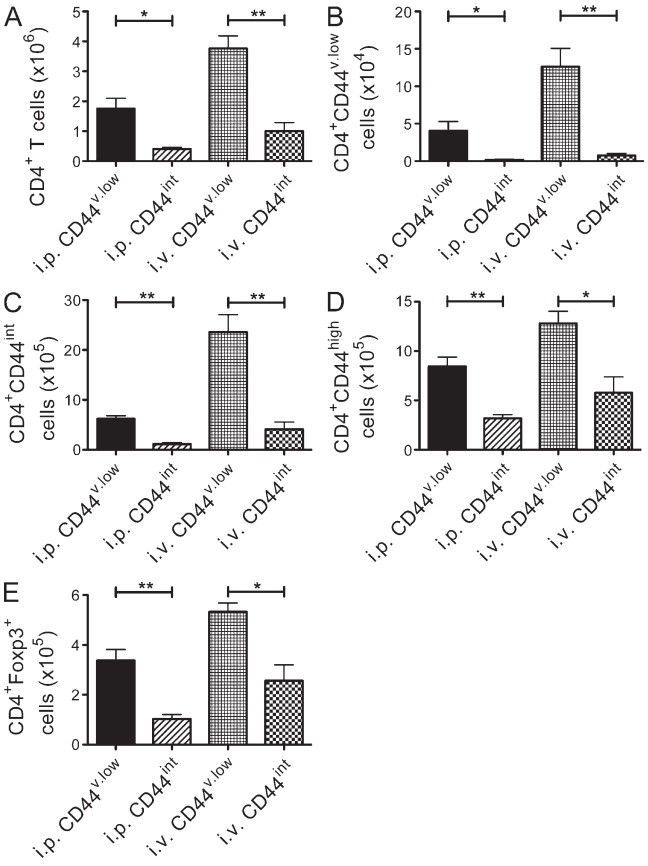

Figure 5. i.v. injection of CD44$^{v.low}$ cells also results in reconstitution of naive and regulatory CD4$^+$ cells. CB17.SCID mice were injected with 2.5 × 10^5 purified CD4$^+$ CD44$^{v.low}$ cells (n = 7) or an equal number of purified CD4$^+$ CD44^{int} cells (n = 7) by the i.p. (n = 4 per group) or i.v. (n = 3 per group) route. Mice were sacrificed 3 wk after cell transfer, and the number of total CD4$^+$ (A), CD44$^{v.low}$ (B), CD44^{int} (C), CD44^{high} (D), and Foxp3$^+$ (E) cells in the spleens determined by FACS. Data are shown as mean ± SEM, and are representative of two independent experiments. Significance between groups is indicated on the figures. *, P = 0.01–0.05; **, P = 0.001–0.01.

Similarly, intracellular measurements of IL-2 on day 3 of culture confirmed that fewer CD4$^+$ CD44$^{v.low}$ cells produced IL-2 than did CD4$^+$ CD44^{int} cells at this time point (Fig. 6 D-F). The percentage of CD4$^+$ CD44$^{v.low}$ cells that expressed cell surface CD25 (63.8% ± 0.7) on the third day of culture was lower than that of CD4$^+$ CD44^{int} cells (73.8% ± 2.4), suggesting that the low levels of IL-2 in the CD4$^+$ CD44$^{v.low}$ cell cultures reflect less efficient secretion rather than increased consumption of the IL-2. Collectively, these data confirm that the CD44$^{v.low}$ cells are functionally naive.

To determine whether the proliferation seen in the CD4$^+$ CD44$^{v.low}$ cell cultures represented many rounds of division of a small proportion of cells, or fewer rounds of division of a large proportion of the cells, proliferation was also measured by CFSE dilution. Thus, purified CD4$^+$ CD44$^{v.low}$ and CD4$^+$ CD44^{int} cells were CFSE labeled, cultured with and without anti-CD3 and anti-CD28 mAb, and analyzed by FACS on

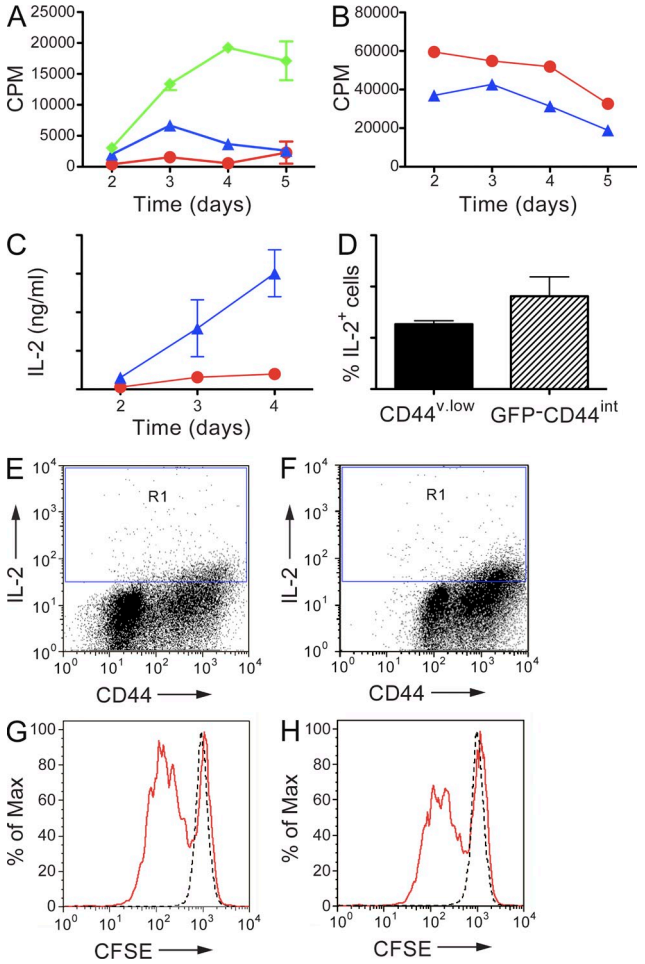

Figure 6. The CD4$^+$ CD44$^{v.low}$ cells are functionally naive. CD4$^+$ Foxp3$^-$ CD44$^{v.low}$ (red) cells, CD4$^+$ Foxp3$^-$ CD44^{int} (blue) cells, and CD4$^+$ Foxp3$^-$ CD44^{high} (green) cells were sorted from GFP-Foxp3 splenocytes and incubated in triplicate at a concentration of 2 × 10^5 cells/ml with anti-CD3 (1 µg/ml) in the absence (A) and presence (B–F) of 1 µg/ml anti-CD28. At 2, 3, 4, and 5 d of culture, the cells were harvested after pulsing for the previous 16 h with [^{3}H]thymidine, and proliferation was measured (A and B). Supernatant was harvested on days 2, 3, and 4, and the concentration of IL-2 was determined by ELISA (C). On day 3 of the culture, wells were pooled and the percentage of IL-2$^+$ cells was determined by FACS (D). Dot plots gated on CD4$^+$ T cells show IL-2 expression in CD4$^+$ CD44$^{v.low}$ cells (E) and CD4$^+$ CD44^{int} cells (F) by intracellular staining. The lower horizontal edge of the box R1 is based on the isotype control staining for anti–IL-2 mAb. The data shown are mean ± SD and are representative of three independent experiments. In a separate experiment, purified CD4$^+$ CD44$^{v.low}$ (G) and CD4$^+$ CD44^{int} (H) cells were labeled with CFSE, cultured in triplicate either with anti-CD3 or anti-CD28 mAb as before or with no stimulation, and analyzed by FACS 3 d later. Stimulated, red; unstimulated, black dotted line. Data shown are representative of three individual cultures and in two independent experiments. Two-way ANOVA showed significance of P < 0001, P < 0.001, and P = 0.0008 for panels A, B, and C, respectively. Groups were compared using Bonferroni's multiple comparison test; in A, CD4$^+$ CD44^{int} is significantly greater than CD4$^+$ CD44$^{v.low}$ on days 3 (P < 0.001) and 4 (P = 0.01–0.05), and CD4$^+$ CD44^{high} is significantly greater than CD4$^+$ CD44^{int} on days 1 (P = 0.01–0.05) 2, 3, and 4 (P < 0.001 for all 3 d). In B, CD4$^+$ CD44$^{v.low}$ is significantly greater than CD4$^+$ CD44^{int} on all days tested (P < 0.001 for all days). In panel C, CD4$^+$ CD44^{int} is significantly greater than CD4$^+$ CD44$^{v.low}$ on days 3 and 4 (P = 0.001–0.01 and P < 0.001, respectively).

days 2 and 3. The percentage of the original cultured cells (precursor frequency) that had divided in response to anti-CD3 and anti-CD28 in both groups was 18.0 ± 1.0% and 33.5 ± 1.2% for the $CD4^+$ $CD44^{v.low}$ cells and 14.9 ± 0.1% and 26.1 ± 1.1% for the $CD4^+$ $CD44^{int}$ cells on days 2 and 3, respectively. The large percentage of divided cells seen in both $CD4^+$ $CD44^{v.low}$ (Fig. 6 G) and $CD4^+$ $CD44^{int}$ (Fig. 6 H) cultures reflects multiple rounds of division from individual precursor cells and was 39.7 ± 1.3% and 78.0 ± 1.3 for the $CD4^+$ $CD44^{v.low}$ cells and 37.8 ± 0.6% and 73.6 ± 1.0% for the $CD4^+$ $CD44^{int}$ cells on days 2 and 3, respectively. Therefore, proliferation seen on day 3 of $CD4^+$ $CD44^{v.low}$ cell cultures represents variable rounds of division by one third of the original cultured cell population.

$CD4^+$ $CD44^{v.low}$ cells show enhanced expression of the survival factors B cell leukemia/lymphoma 2 (Bcl-2) and CD127

Expression of high levels of the antiapoptotic factor Bcl-2 (Mueller et al., 1996) and the IL-7 receptor CD127 (Sudo et al., 1993) is associated with prolonged T cell survival. In splenocytes from untreated mice, a significantly higher percentage of $CD4^+$ $CD44^{v.low}$ cells expressed Bcl-2 than either $CD4^+$ $CD44^{int}$ cells or $CD4^+$ $CD44^{high}$ cells (Fig. 7 A). Moreover, the density of expression of Bcl-2 in $Bcl\text{-}2^+$ cells was significantly greater in $CD4^+$ $CD44^{v.low}$ cells than in $Bcl\text{-}2^+$ cells from either of the other two cell populations (Fig. 7 B).

We next examined expression of Bcl-2 in cells expanded in SCID mice. Mice were injected with purified $CD4^+$ $CD44^{v.low}$ cells or $CD4^+$ $CD44^{int}$ cells, and the expression of Bcl-2 in the reconstituted $CD4^+$ T cell subsets was determined. A significantly greater percentage of $CD4^+$ $CD44^{v.low}$ cells expressed Bcl-2 than $CD4^+$ $CD44^{int}$ and $CD4^+$ $CD44^{high}$ cells, whether they were derived from $CD4^+$ $CD44^{v.low}$, $CD4^+$ $CD44^{int}$ cells, or from cells isolated from untreated BALB/c mice (Fig. 7 C). In addition, the percentage of $CD4^+$ $CD44^{high}$ cells that expressed Bcl-2 was significantly greater when derived from $CD4^+$ $CD44^{v.low}$ cells than when derived from $CD4^+$ $CD44^{int}$ cells (Fig. 7 D), which is consistent with the development of long-term memory cells.

A greater percentage of $CD4^+$ $CD44^{v.low}$ cells expressed the IL-7 receptor CD127 than $CD4^+$ $CD44^{int}$ cells in untreated control BALB/c mice (Fig. 7 E). After reconstitution of mice, CD127 was expressed on a significantly smaller percentage of total $CD4^+$ T cells when derived from $CD4^+$ $CD44^{v.low}$ cells, compared with total $CD4^+$ T cells from mice infused with $CD4^+$ $CD44^{int}$ cells (Fig. 7 F). However, the absolute number of $CD4^+$ T cells expressing CD127 was significantly greater in recipients of $CD4^+$ $CD44^{v.low}$ cells than in mice that received $CD4^+$ $CD44^{int}$ cells (Fig. 7 G).

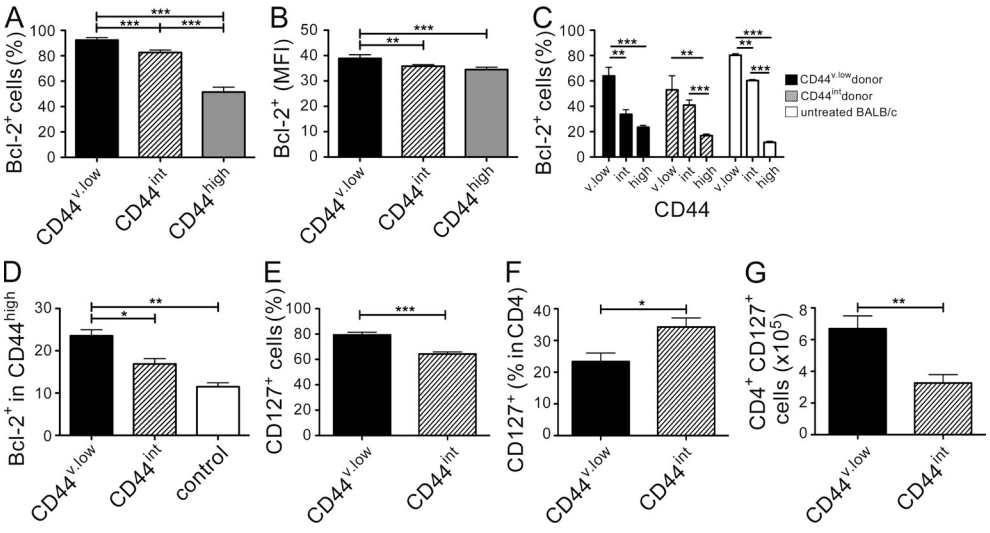

Figure 7. $CD4^+$ $CD44^{v.low}$ cells show enhanced expression of survival factors Bcl-2 and CD127. Splenocytes from untreated BALB/c mice ($n = 4$), CB17.SCID mice reconstituted 3 wk earlier with sorted $CD4^+$ $CD44^{v.low}$ cells ($n = 6$), or an equal number of $CD4^+$ $CD44^{int}$ cells ($n = 6$), were co-stained with mAbs specific for CD4, CD44, and Bcl-2 (A–D) or CD127 (E–G). (A and B) The percentage of $Bcl\text{-}2^+$ $CD4^+$ T cell subsets (A) and the mean fluorescence intensity of Bcl-2 in $Bcl\text{-}2^+$ cells (B) in untreated BALB/c mice are shown. (C) The percentage of $Bcl\text{-}2^+$ cells in the indicated subsets in mice reconstituted with $CD4^+$ $CD44^{v.low}$ cells (black bars), $CD4^+$ $CD44^{int}$ cells (hatched bars), or in untreated BALB/c mice (white bars). (D) The percentage of $Bcl\text{-}2^+$ $CD44^{high}$ $CD4^+$ memory cells in mice reconstituted with $CD4^+$ $CD44^{v.low}$ cells (black bar), $CD4^+$ $CD44^{int}$ cells (hatched bar), or in untreated BALB/c mice (white bar). (E and F) The percentage of $CD127^+$ $CD4^+$ $CD44^{v.low}$ cells and $CD4^+$ $CD44^{int}$ cells in untreated BALB/c splenocytes (E), and the percentage (F) and total number (G) of $CD127^+$ $CD4^+$ T cells in mice reconstituted with $CD4^+$ $CD44^{v.low}$ cells (black bars) or $CD4^+$ $CD44^{int}$ cells (hatched bars) is shown. Data are shown as mean ± SD, and are representative of two independent experiments. One-way ANOVA showed significance of $P < 0001$ for A, B, and D; $P < 0.001$, $P = 0.0085$, and $P < 0.0001$ for $CD4^+$ $CD44^{v.low}$, $CD4^+$ $CD44^{int}$, and untreated BALB/c groups, respectively. $P = 0.0013$ for panel C. Significance between groups using Bonferroni's multiple comparison test is indicated on the figures. *, $P = 0.01–0.05$; **, $P = 0.001–0.01$; ***, $P < 0.001$.

$CD4^+$ $CD44^{v.low}$ cells express a higher density of CD5 than $CD4^+$ $CD44^{int}$ cells

Cell surface expression of CD5 is proportional to the TCR signaling capacity of that cell in response to self-peptide/MHC (Azzam et al., 1998), whereas a high surface density of TCR (Kassiotis et al., 2003) and CD4 (Strong et al., 2001) can increase T cell avidity for APC. The density of CD5 expression on $CD4^+$ $CD44^{v.low}$ cells was significantly higher than that on $CD4^+$ $CD44^{int}$ cells (Fig. 8 A), whereas expression of TCR (Fig. 8 B), CD4 (Fig. 8 C), and CD3 (Fig. 8 D) were similar between the two cell subsets.

T cell receptor repertoire diversity is significantly greater in $CD4^+$ T cells derived from $CD4^+$ $CD44^{v.low}$ cells than in cells derived from $CD4^+$ $CD44^{int}$ cells

The complementary determining region 3 (CDR3) of the TCR confers antigen specificity (Jorgensen et al., 1992), and can vary in size depending on the number of nucleotides removed or added during rearrangement of TCR genes (Pannetier, 1993; Pannetier et al., 1995). The probability of distribution of various CDR3 sizes provides a CDR3 spectratype, or pattern of peaks, which is Gaussian in the absence of clonal expansion (i.e. maximum diversity; Pannetier, 1993). Perturbation of CDR3 spectratypes away from Gaussian can then be used as an indication of TCR repertoire diversity; the lower the perturbation, the greater the diversity. The peaks in a CDR3 spectratype are given numerical values by determining the contribution of each peak to the total area under all peaks measured, where the sum of all peaks measured is 100%. The percentage of perturbation of a peak generated from an experimental cell subset is calculated as the difference between the value given to that peak and the value given to the corresponding peak for a control cell subset that shows a Gaussian distributed CDR3 spectratype (no clonal expansion). Experimental peaks with an area greater than control peaks will have positive values (positive perturbation). The sum of all positive perturbation (total positive perturbation) for all peaks within a CDR3 spectratype is the perturbation for that TCR Vβ CDR3 spectratype. The mean CDR3 spectratype perturbation for all TCR Vβ tested gives the overall sample perturbation shown in Fig. 9. Significant perturbation in the spectratype reflects clonal expansion within that Vβ family.

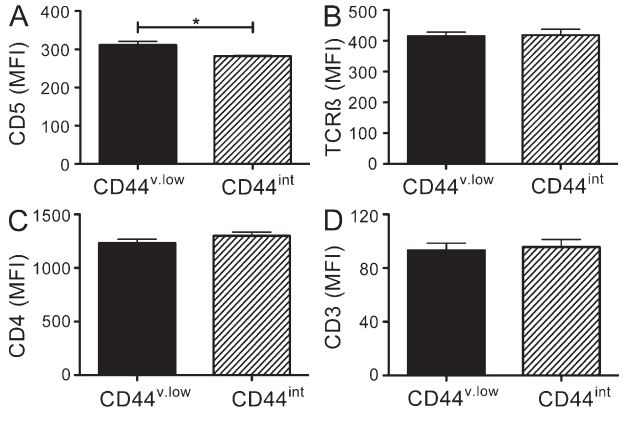

Figure 8. $CD4^+$ $CD44^{v.low}$ cells express a higher density of CD5 than $CD4^+$ $CD44^{int}$ cells. Splenocytes isolated from untreated BALB/c mice ($n = 3$) were co-stained with mAbs specific for CD4 and CD44 and CD5 (A), TCR (B), CD4 (C), or CD3 (D). The mean fluorescence intensity (MFI) of CD5, TCR, CD4, and CD3 on $CD4^+$ $CD44^{v.low}$ and $CD4^+$ $CD44^{int}$ cells was determined by FACS. Data are shown as mean ± SD and are representative of four independent experiments for CD5 and three independent experiments for TCR, CD4, and CD3. The two-tailed unpaired Student's *t* test showed a significantly greater CD5 MFI on $CD4^+$ $CD44^{v.low}$ cells than on $CD4^+$ $CD44^{int}$ cells ($P = 0.01–0.05$)

We hypothesized that cells derived from $CD4^+$ $CD44^{v.low}$ cells might possess a greater TCR repertoire than cells derived from other naive and memory cells. To test this, we examined CDR3 spectratypes from the initial cells transferred, as well as from the in vivo–expanded populations. The CDR3 spectratypes for TCR Vβ1, 2, 4, 6, 7, 8.1, 8.2, 8.3, 10, 14, and 15 for $CD4^+$ T cells sorted from untreated BALB/c mice were determined and used as standard control spectratypes showing Gaussian distribution. We initially examined CDR3 spectratypes for each Vβ family in $CD4^+$ $CD44^{v.low}$, $CD4^+$ $CD44^{int}$, and $CD4^+$ $CD44^{high}$ cells sorted from untreated BALB/c mice. The overall sample perturbation was shown to be between 4 and 6% for all $CD4^+$ cell subsets tested (Fig. 9 A), demonstrating that the diversity of the TCR repertoire, as measured by this assay, is similar in the three $CD4^+$ T cell populations isolated from untreated mice. This is also shown by the near Gaussian distribution of the CDR3 spectratypes in total $CD4^+$, $CD4^+$ $CD44^{v.low}$, $CD4^+$ $CD44^{int}$, and $CD4^+$ $CD44^{high}$ cells (Fig. 9 B).

To test the hypothesis that the diversity of the T cell repertoire derived from $CD4^+$ $CD44^{v.low}$ cells is greater than that derived from $CD4^+$ $CD44^{int}$ cells, $CD4^+$ T cells were purified from SCID mice that had been infused with either $CD4^+$ $CD44^{v.low}$ cells, or with $CD4^+$ $CD44^{int}$ cells. $CD4^+$ T cells isolated from mice infused with $CD4^+$ $CD44^{high}$ cells were also included as a positive control because memory cells show evidence of clonal expansion after lymphopenia-induced proliferation (Eyrich et al., 2002). The data in Fig. 9 C show significant spectratype perturbation in $CD4^+$ T cells purified from all three groups of SCID recipients, reflecting evidence of clonal expansion. However, the overall perturbation of $CD4^+$ T cells derived from $CD4^+$ $CD44^{v.low}$ cells ($17 \pm 8\%$) is significantly less than that for either $CD4^+$ $CD44^{int}$ ($25 \pm 10\%$) or $CD4^+$ $CD44^{high}$ ($32 \pm 16\%$) cells (Fig. 9 C). Fig. 9 D shows a representative CDR3 spectratype for TCR Vβ10 in total $CD4^+$ T cells, $CD4^+$ $CD44^{v.low}$, $CD4^+$ $CD44^{int}$, and $CD4^+$ $CD44^{high}$ cells. Although the $CD4^+$ $CD44^{v.low}$ cells show a partial Gaussian distribution of the CDR3 products with different lengths, $CD4^+$ $CD44^{int}$ and $CD4^+$ $CD44^{high}$ cells do not. These data indicate a greater diversity in the TCR repertoire derived from $CD4^+$ $CD44^{v.low}$ cells compared with either $CD4^+$ $CD44^{int}$ and $CD4^+$ $CD44^{high}$ cells.

The ability to reconstitute a $CD4^+$ T cell pool with a diverse TCR repertoire would predict proliferation of a large proportion of the $CD4^+$ $CD44^{v.low}$ cells on transfer into

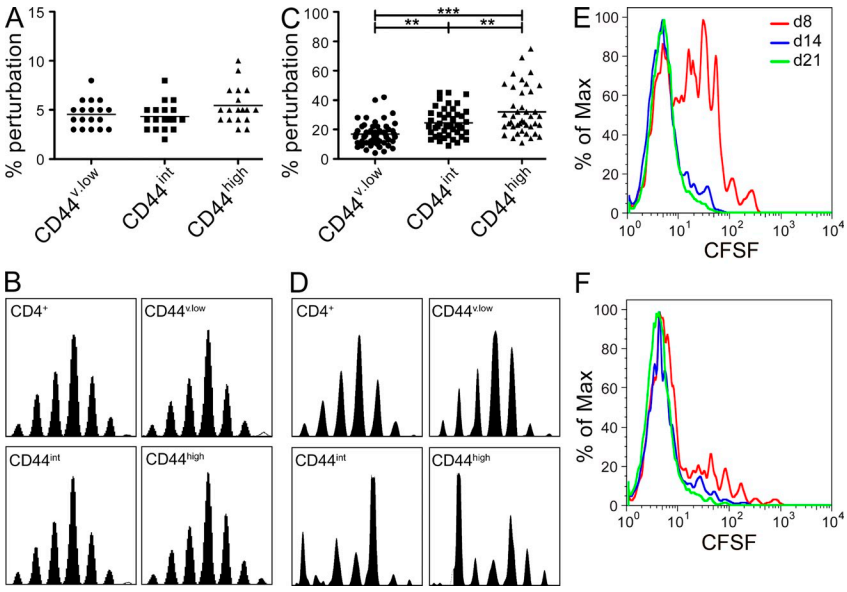

Figure 9. T cell receptor repertoire diversity is significantly greater in CD4+ T cells derived from CD4+ CD44v.low cells than in cells derived from CD4+ CD44int cells. CD4+ CD44v.low ($n = 2$), CD4+ CD44int ($n = 2$), and CD4+ CD44high ($n = 2$) cells were sorted from BALB/c splenocytes, and an equal number of each subset (10^6) was used to determine the TCR Vβ perturbation of the CDR3 spectratype. (A) The overall sample perturbation (% perturbation) includes the perturbation of TCR Vβ1, 2, 4, 6, 7, 8.1, 8.2, 8.3, 10, 14, and 15 for each cell subset. The CDR3 spectratype profile for each subset is shown for Vβ10 (B). In a separate experiment, CD4+ cells from individual mice were either enriched or sorted from CB17.SCID mice that were injected 3 wk earlier with 2.5×10^5 sorted CD4+ CD44v.low ($n = 5$), CD4+ CD44int ($n = 5$), or CD4+ CD44high ($n = 5$) cells. Either 5×10^5 enriched cells or $2.4–3.0 \times 10^5$ sorted cells were used for CDR3 spectratype analysis. (C) The total perturbation for each of the TCR Vβ tested in each CD4+ T cell subset was determined. In A and C, the dots represent the perturbation for each TCR Vβ tested in each individual mouse, and the horizontal line represents the mean of all TCR Vβ tested for all mice in each group. The CDR3 spectratype profile for TCR Vβ10 is shown for total CD4+ T cells and all CD4+ T cell subsets tested (D). The experiment was performed three times, and the data shown are pooled from all three independent experiments. (E and F) 2.5×10^5 sorted CFSE-labeled CD4+ CD44v.low cells ($n = 9$) or CD4+ CD44int cells ($n = 9$) were infused into CB17.SCID recipients. CFSE intensity in CD4+ splenocytes was determined on days 8 ($n = 3$), 14 ($n = 3$), and 21 ($n = 3$) after cell infusion. Histograms show representative examples of the CFSE intensity in CD4+ splenocytes from CD4+ CD44v.low-infused (E) or CD4+ CD44int-infused (F) mice at each time point. The data are representative of two independent experiments. One-way ANOVA showed significance of $P < 0001$ for C. Significance between groups using Bonferroni's multiple comparison test is indicated on the figures. **, $P = 0.001–0.01$; ***, $P < 0.001$.

CB17.SCID mouse recipients. To test this, sorted CD4+ CD44v.low cells and CD4+ CD44int cells were labeled with CFSE and infused into CB17.SCID mouse recipients as before. By day 8 after infusion, the majority of CD4+ cells from spleens of mice infused with CD4+ CD44v.low cells had divided between 3 and 6 times (Fig. 9 E). In general, proliferation of the CD4+ CD44int population was more extensive at this time point, with the majority of infused cells dividing more than 6 times in most of the recipient mice (Fig. 9 F). By days 14 and 21 after cell infusion, over 90% of the infused cells in all of the mice in both groups had divided >7 times (Fig. 9, E and F) suggesting that the majority of the CD44v.low population contribute to the reconstitution of CD4+ T cells in SCID mouse recipients.

DISCUSSION

The functional importance of the CD4+ CD44v.low cell population was suggested by their ability to significantly delay the onset of cachexia and lymphopenia in mice with a profound tumor burden (Wang et al., 2008). Although lymphopenia can also be overcome by proliferation and differentiation of naive and memory cells (Freitas and Rocha, 2000; Jameson, 2002; Wu et al., 2004), neither CD4+ CD44int naive cells nor memory CD4+ T cells inhibit cachexia-associated lymphopenia, suggesting that the CD4+ CD44v.low cell subset might be the dominant peripheral CD4+ T cell precursor population in a cachexic environment. Here, we extend these findings to show that the CD4+ CD44v.low cell subset expands and differentiates into naive, memory, and Foxp3+ regulatory CD4+ T cell subsets having a diverse TCR repertoire. Moreover, their ability to reconstitute the CD4+ T cell pool is independent of cachexia, indicating the potential importance in enhancing CD4+ CD44v.low cell numbers and function to treat drug- and disease-induced lymphopenia.

Using a cell transfer model in which highly purified CD4+ T cell subsets were infused into immunodeficient SCID mice, we have found that CD4+ CD44v.low cells more efficiently generate large numbers of CD4+ T cells in immunodeficient recipients than other naive or memory CD4+ cells. Moreover, the ratio between naive and memory cells in mice reconstituted by CD4+ CD44v.low cells is the same as that seen in untreated wild-type mice, suggesting that the repopulated cells are under homeostatic equilibrium. In addition, we showed that a significantly greater percentage of memory cells derived from CD4+ CD44v.low cells express Bcl-2 than memory cells derived from CD4+ CD44int cells, suggesting they may exhibit the survival characteristics of long-lived memory cells. Long-lived memory cells are derived from naive cells that experience strong antigen stimulation during the primary response to exogenous antigen (Williams et al., 2008), and this is consistent with our finding that CD4+ CD44v.low cells express a high density of CD5, which is a characteristic of cells with high TCR signaling capacity for self-peptide/MHC (Azzam et al., 1998). CD4+ CD44v.low cells also express high levels of Bcl-2 (Mueller et al., 1996), as well as CD127, the IL-7 receptor (Sudo et al., 1993), which is consistent with

a survival advantage for $CD4^+$ $CD44^{v.low}$ cells leading to efficient accumulation in vivo.

The ability of $CD4^+$ $CD44^{v.low}$ cells to generate a naive $CD4^+$ T cell pool in profoundly lymphopenic hosts challenges the current paradigm that the naive cell compartment can only be reconstituted by thymopoiesis (Ge et al., 2002). This paradigm was originally based on the finding that although naive cells rapidly differentiate into memory phenotype cells when infused into irradiated hosts (Ernst et al., 1999: Goldrath and Bevan, 1999), they were unable to reconstitute the naive cell compartment (Greenberg and Riddell, 1999). A later study countered that by suggesting that naive T cells could reconstitute irradiated mice with cells of both naive and memory phenotype, and that the naive cells were derived from cells that transiently expressed the memory phenotype (Goldrath et al., 2000). Finally, Ge et al. (2002) have shown that the previous findings might be explained by lymphoid stem cells present in the cell injection, and that naive cell reconstitution could not be achieved with purified naive T cells alone. In their study, Chen et al. further showed that naive cell reconstitution was thymus dependent, which confirmed the prevailing paradigm that the naive cell compartment can only be reconstituted by thymopoiesis. Our data challenge this paradigm by identifying a novel peripheral CD4 T cell subset ($CD44^{v.low}$ cells) that can reconstitute the naive cell compartment in thymectomized SCID mice.

The $Foxp3^+$ regulatory cell subset Tregs (Fontenot and Rudensky, 2005; Mucida et al., 2005) play a role in maintaining a healthy immune system by limiting undesirable immune responses. Tregs can be divided into two major subsets on the basis of their development, natural and acquired, and constitute 5–10% of total $CD4^+$ T cells in healthy BALB/c mice. Natural Tregs (nTregs) are thought to be a separate, thymus-derived lineage of T cells (Fontenot et al., 2003; Khattri et al., 2003), whereas aquired Tregs (aTregs) can be generated from naive $CD4^+$ $Foxp3^-$ T cells in the periphery (Apostolou and von Boehmer, 2004; Kretschmer et al., 2005). Tregs are undetectable within the $CD4^+$ $CD44^{v.low}$ cell population, but are readily detectable within the $CD4^+$ $CD44^{int}$ and $CD4^+$ $CD44^{high}$ cells. $CD4^+$ $CD44^{int}$ cells that are experimentally depleted of $Foxp3^+$ cells are inefficient in generating a $Foxp3^+$ population during lymphopenia-induced proliferation. In sharp contrast, $CD4^+$ $CD44^{v.low}$ cells readily differentiate to express Foxp3 during homeostatic reconstitution, with >10% of $CD4^+$ $CD44^{v.low}$-derived cells expressing Foxp3 by 3 wk after transfer into SCID recipients. Approximately $2–6 \times 10^5$ $CD4^+$ $Foxp3^+$ cells are generated from the original 2.5×10^5 $CD4^+$ $CD44^{v.low}$ cells transferred. Because it is unlikely that this large number of $Foxp3^+$ cells was derived from proliferation of a small undetectable $Foxp3^+$ population present in the original $CD4^+$ $CD44^{v.low}$ cell infusion, the data strongly suggest conversion of $CD4^+$ $CD44^{v.low}$ $Foxp3^-$ cells to aTregs. Regardless of the exact mechanism, our data suggest that $CD4^+$ $CD44^{v.low}$ cells are the main precursor population for the generation of Tregs.

The absence of $Foxp3^+$ regulatory cells in the $CD4^+$ $CD44^{v.low}$ cell population that reconstituted $CD4^+$ cells when transferred in lymphopenic hosts, might suggest the potential for autoimmunity in the expanded population (Haribhai et al., 2009). However, we found no evidence of autoimmunity in SCID mice injected with purified $CD4^+$ $CD44^{v.low}$ cells (our unpublished data). It is possible that conversion of $CD4^+$ $CD44^{v.low}$ $Foxp3^-$ cells to aTregs prevents the development of autoimmunity. Alternatively, because CD5 is known to be a negative regulator for TCR signaling (Brossard et al., 2003), and plays a role in protection from activation-induced cell death (Friedlein et al., 2007), its higher expression on $CD4^+$ $CD44^{v.low}$ cells might allow efficient accumulation of these cells in vivo while suppressing the potential for autoimmunity. Such a possibility has been described for other cell populations that express a high density of CD5 (Kassiotis et al., 2003; Dalloul, 2009).

In addition to recognition of self-peptide/MHC (Viret et al., 1999; Moses et al., 2003), lymphopenia-induced proliferation of naive cells requires the survival cytokine, IL-7 (Maraskovsky et al., 1996; Tan et al., 2001). Signaling in response to IL-7 results in down-regulation of its own receptor, CD127, thus limiting the expansion of IL-7–stimulated clones without limiting the expansion of the cell population as a whole, and maintaining TCR diversity (Park et al., 2004). Our data show that after expansion in vivo, the percentage of $CD4^+$ T cells that express CD127 is reduced to a significantly greater extent on $CD4^+$ T cells derived from $CD4^+$ $CD44^{v.low}$ than it is on cells derived from $CD4^+$ $CD44^{int}$ cells, predicting less clonal expansion and greater TCR diversity in the former. Indeed, we found that the TCR repertoire generated by $CD4^+$ $CD44^{v.low}$ cells is significantly greater than that generated by $CD4^+$ $CD44^{int}$ cells. The finding that the majority of the $CD4^+$ $CD44^{v.low}$ cells divide in SCID mice in vivo is consistent with the notion that a large proportion of the infused cells contribute to the reconstitution and diversity of the TCR repertoire. The diversity of the $CD4^+$ TCR repertoire derived form naive $CD4^+$ $CD44^{int}$ cells is significantly greater than that seen for $CD4^+$ T cells derived from memory $CD4^+$ T cells, and this is consistent with published data that compares the TCR diversity in $CD4^+$ T cells derived from naive and memory cells (Eyrich et al., 2002).

Proliferation of $CD4^+$ $CD44^{v.low}$ cells in response to anti-CD3 stimulation in vitro is dependent on co-stimulation, identifying them functionally as naive $CD4^+$ T cells (Croft and Dubey, 1997). Furthermore, they are more dependent on co-stimulation than $CD4^+$ $CD44^{int}$ naive cells, and secrete significantly less IL-2 than their $CD4^+$ $CD44^{int}$ naive cell counterparts. These observations suggest that $CD4^+$ $CD44^{v.low}$ cells may represent the most naive population within the total naive cell subset. Importantly, $CD4^+$ $CD44^{v.low}$ cells are not recent thymic emigrants because they do not express the characteristic patterns of CD3, CD127, CD28, CD45RB, and CD31 (unpublished data) that have been used to define recent thymic emigrants (Jores and Meo, 1993; Kimmig et al., 2002; Boursalian et al., 2004).

In summary, this study further describes the properties of a new $CD4^+$ T cell subset, the $CD4^+$ $CD44^{v.low}$ cells. This cell subset has all of the phenotypic and functional characteristics of naive $CD4^+$ T cells. Its unique ability to repopulate naive, memory, and $Foxp3^+$ regulatory $CD4^+$ T cell subsets with a diverse TCR repertoire, independent of the thymus, indicate its role as a peripheral precursor responsible for maintaining immune integrity. Strategies that promote $CD4^+$ $CD44^{v.low}$ cell numbers and/or function might therefore be critical for the treatment of lymphopenia and lymphopenia-associated disease.

MATERIALS AND METHODS

Mice. Euthymic and thymectomized CBySmn.CB17-$Prkdc^{scid}$/J mice (CB17.SCID) and BALB/cByJ (BALB/c) mice were purchased from The Jackson Laboratory. As a standard precaution, at the end of each experiment involving thymectomized mice, fibrous and fatty tissue remaining at the site of surgery was removed and analyzed by FACS for the presence $CD3^+$ cells to confirm complete thymectomy. $Foxp3^{EGFP}$ mice (Foxp3-GFP) on the BALB/c background were a gift from T. Chatila (University of California, Los Angeles, Los Angeles, CA), and bred at the Torrey Pines Institute for Molecular Studies. Mice were maintained under specific pathogen–free conditions and used between 8–20 wk of age. All experiments were approved by the Torrey Pines Institute for Molecular Studies Institutional Animal Care and Use Committee.

Phenotypic analysis by FACS. mAbs specific for CD4 (RM4-5 conjugated to either allophycocyanin [APC] or PE-Cy7), CD8α (53–6.7 conjugated to APC), CD44 (IM7 conjugated to either PE or APC), CD5 (53–7.3 conjugated to FITC), TCRβ (H57−597 conjugated to APC), CD3 (145-2C11, conjugated to either FITC or PE), CD45RB (16A conjugated to PE), CD25 (PC61 conjugated to PE-Cy7), CD28 (37.51 conjugated to PE), CD31 (MEC13.3 conjugated to FITC), and IL-2 (JES6-5H4 conjugated to PE) were purchased from BD. mAbs specific for Foxp3 (FJK-16s conjugated to FITC) and CD127 (A7R34 conjugated to PE-Cy7) were purchased from eBioscience. Bcl-2 expression was determined using the FITC Anti–Mouse Bcl-2 Set following manufacturer's instructions (BD). All experiments included relevant isotype controls. Cells were acquired on a FACSCalibur and analyzed using either CellQuest version 3.3 (BD) or FlowJo version 8.8.6 (Tree Star, Inc.).

Cell subset purification. $CD4^+$ cells were enriched from splenocytes by negative selection using magnetic beads (MACS $CD4^+$ T cell isolation kit; Miltenyi Biotec). Enriched (70–75%) $CD4^+$ cells were labeled with APC- and PE-conjugated CD4 and CD44 mAbs, respectively, and purified to >99% by sorting on a FACSAria or FACSDIVA (BD). For the purpose of sorting, $CD4^+$ $CD44^{v.low}$ cells were considered those within the 3% of $CD4^+$ cells with the lowest CD44 density, the $CD4^+$ $CD44^{int}$ cells were the 30% of $CD4^+$ cells spanning the CD44 intermediate peak, and the $CD4^+$ $CD44^{high}$ cells were considered the 5–10% of $CD4^+$ cells with the highest density of CD44 (Fig. S2). The $CD4^+$ $CD44^{v.low}$-depleted cells were purified by depleting the 20% $CD4^+$ cells with the lowest density of CD44 by sorting. $CD4^+$ $Foxp3^-$ cells were purified from Foxp3-GFP splenocytes after labeling with APC-conjugated anti-CD4 and sorting $CD4^+$ GFP^- (Foxp3-depleted) cells.

Adoptive transfer. Sorted cells were washed once in PBS, and between 2.0×10^5 and 2.5×10^5 cells were infused into recipients in 100 µl PBS. Mice were infused with $CD4^+$ cell subsets by i.p. injection, except in one experiment where i.p. injection is compared directly with i.v. injection. In some experiments, sorted cells were labeled with CFSE (Invitrogen) using the standard published protocol (Lyons and Parish, 1994) before infusion, and their proliferation was measured by CFSE dilution.

In vitro proliferation and IL-2 measurements. Sorted $CD4^+$ subsets were incubated in 96-well plates at a concentration of 4×10^4 cells per well. Cultures were stimulated with plate-bound anti-CD3 (145-2C11) and anti-CD28 (37.51) mAb (BD) at 1 µg/ml for 2, 3, 4, and 5 d (a different plate for each time point) in RPMI culture medium (Invitrogen) with 5% fetal bovine serum (InterGen), Hepes (Invitrogen), glutamine, penicillin, streptomycin (Irvine Scientific), and 2-mercaptoethanol (Sigma-Aldrich). To measure proliferation, cells were pulsed with [^{3}H]thymidine (0.5 µCi/well; GE Healthcare), and harvested 16 h later. Incorporation of [^{3}H]thymidine was measured on a scintillation β-counter (Wallac; PerkinElmer). In other experiments, sorted cells were labeled with CFSE (Invitrogen) using the standard published protocol (Lyons and Parish, 1994) before culture, and their proliferation was measured by CFSE dilution. Precursor frequency was calculated using FlowJo version 8.8.6 (Tree Star, Inc.). IL-2 content in cultured cells was determined by intracellular stain and FACS, and in the culture supernatant by ELISA.

Analysis of TCR repertoire modifications by CDR3 spectratyping. Random rearrangement of TCR variable (V), diversity (D), joining (J), and constant (C) region results in enormous diversity in the TCR repertoire (Pannetier, 1993; Jores and Meo, 1993). In this study, the CDR3 spectratype for V-C combinations in eleven different TCR Vβ families (BV-BC repertoire) was used to compare the diversity of the TCR repertoire in different $CD4^+$ T cell subsets. The perturbation of the BV-BC repertoire for each Vβ family in $CD4^+$ T cell populations after homeostatic and lymphopenia-induced proliferation was compared with unstimulated $CD4^+$ T cells (Gorochov et al., 1998; Han et al., 1999). The mean BV-BC perturbation for all TCR Vβ tested is calculated to give the overall sample perturbation tested, and this is compared between cell subsets.

Typically, the CDR3 spectratype from unstimulated $CD4^+$ T cells consists of six or seven discrete and easily identifiable peaks (Fig. 9, B and D, for $CD4^+$ cells). The area under each peak for a given TCR Vβ is determined using GeneMapper Software, and the contribution of each peak to the total area under all peaks for that TCR Vβ family is calculated as a percentage. This is shown for Vβ10 in Table S2. The CDR3 spectratype is constant in unstimulated $CD4^+$ T cells isolated from different BALB/c mice (Table S3), and is also unaffected by differences in the cell number used for RNA isolation if between 10^5 and 10^6 (Table S4). The CDR3 spectratype for each experimental cell subset was compared with that of the unstimulated control cells (Table S5). The perturbation for each TCR Vβ peak is the difference between the percent value given to the control peak and the percent value given to the corresponding experimental peak. Experimental peaks with an area greater, and lower, than control peaks will have positive values (positive perturbation) and negative (negative perturbation) values, respectively. The sum all positive perturbation (total positive perturbation) for each TCR Vβ family is calculated, and the mean for all TCR Vβ tested gives the overall sample perturbation shown in Fig. 9. It is important to note that the total positive perturbation is equal to the total negative perturbation.

Protocol used to generate product for CDR3 spectratyping. Total RNA was extracted from highly purified $CD4^+$ T cell subsets using the RNeasy Mini kit (QIAGEN). cDNA was synthesized using oligo (dT) 12–18 superscript reverse transcription (Invitrogen) at 42°C for 50 min (min) followed by 15 min at 70°C. PCR amplification of newly synthesized cDNA was performed in a mixture containing 0.75 U of AmpliTaq DNA Polymerase (Applied Biosystems), 1.5 mM $MgCl_2$, 0.25 mM dNTP, and 0.5 µM Cβ145 primer with Vβ1, 2, 4, 6, 7, 8.1, 8.2, 8.3, 10, 14, and 15 primers (primer sequences are listed in Table S6) for 2 min at 94°C, followed by 39 cycles of 45 s at 94°C, 45 s at 60°C, 45 s at 72°C, and finally 10 min at 72°C. Run-off reactions were performed with 0.04 µM of a Cβ5-specific FAM-labeled primer in a mixture of Taq DNA polymerase (New England BioLabs), 3 mM $MgCl_2$, and 0.2 mM dNTP for 11 s at 94°C, followed by 15 cycles of 45 s at 94°C, 45 s at 55°C, 1 min at 72°C, and finally 5 min at 72°C. All PCR reactions were performed on a 96-well GeneAmp PCR System 9700 (Applied Biosystems). Run-off products were denatured in deionized formamide with a GeneScan HD (ROX; Applied Biosystems) size standard (Applied Biosystems). The mixture was incubated for 2 min at 94°C and cooled on ice for 5 min. Fragment analysis of the denatured products was

performed using ABI Prism 3100 CE device with GeneMapper Software V4.0 (Applied Biosystems).

Statistical analysis. Statistical analysis to compare $CD4^+$ cell subset reconstitution, expression of Bcl-2, and percentage of perturbation of the CDR3 spectratype, was performed using one-way analysis of variance (ANOVA), followed by the Bonferroni multiple comparison test. Comparisons between reconstitution by two cell subsets in thymectomized and euthymic mice, and by intravenous and peritoneal injection, were performed using the Student's *t* test. Comparison of CD5, TCRβ, CD4, CD3, and CD127 expression and cell division based on CFSE dilution was performed using the unpaired Student's *t* test. Comparison of proliferation, IL-2 production, and IL-2 secretion was performed using two-way ANOVA, followed by the Bonferroni multiple comparison test. A p-value <0.05 is considered significant. Significance is determined using the data presented in each figure.

Online supplemental material. Fig. S1 shows the percentage of $CD4^+$ $CD44^{v.low}$, $CD4^+$ $CD44^{int}$, and $CD4^+$ $CD44^{high}$ cells that express Foxp3. Fig. S2 shows CD44 expression on $CD4^+$ $CD44^{v.low}$, $CD4^+$ $CD44^{int}$, and $CD4^+$ $CD44^{high}$ cells before and after sorting. Table S1 shows that $CD4^+$ $Foxp3^+$ cells can be found in the $CD4^+$ $CD44^{int}$ and $CD4^+$ $CD44^{high}$ subsets, but not in the $CD4^+$ $CD44^{v.low}$ subset. Table S2 shows how the percentage contribution of each spectratype peak within a Vβ family is calculated, using VB10 as an example. Table S3 shows that the contribution of each spectratype peak within a Vβ family is consistent in $CD4^+$ T cells isolated from three individual untreated BALB/c mice, using Vβ10 as an example. Table S4 shows that the distribution of CDR3 regions with different lengths within a Vβ family does not change if the number of $CD4^+$ T cells analyzed at one time is between 10^5 and 10^6. Table S5 shows the strategy used to calculate the total perturbation of each TCR Vβ family using Vβ 10 as an example. Table S6 shows the sequence of mouse Vβ and Cβ primers used for immunoscope analysis. Online supplemental material is available at http://www.jem.org/cgi/content/full/jem.20100598/DC1.

Funding for this study was provided by grants from the Diabetes National Research Group (DNRG5304), the Alzheimer's and Ageing Research Center (AARC5105), and the National Institutes of Health (CA109729) to J.D. Davies.

The authors have no conflicting financial interests.

Submitted: 25 March 2010
Accepted: 9 November 2010

REFERENCES

Apostolou, I., and H. von Boehmer. 2004. In vivo instruction of suppressor commitment in naive T cells. *J. Exp. Med.* 199:1401–1408. doi:10.1084/jem.20040249

Azzam, H.S., A. Grinberg, K. Lui, H. Shen, E.W. Shores, and P.E. Love. 1998. CD5 expression is developmentally regulated by T cell receptor (TCR) signals and TCR avidity. *J. Exp. Med.* 188:2301–2311. doi:10.1084/jem.188.12.2301

Bell, E.B., and S.M. Sparshott. 1997. The peripheral T-cell pool: regulation by non-antigen induced proliferation? *Semin. Immunol.* 9:347–353. doi:10.1006/smim.1997.0092

Bottomly, K., M. Luqman, L. Greenbaum, S. Carding, J. West, T. Pasqualini, and D.B. Murphy. 1989. A monoclonal antibody to murine CD45R distinguishes CD4 T cell populations that produce different cytokines. *Eur. J. Immunol.* 19:617–623. doi:10.1002/eji.1830190407

Boursalian, T.E., J. Golob, D.M. Soper, C.J. Cooper, and P.J. Fink. 2004. Continued maturation of thymic emigrants in the periphery. *Nat. Immunol.* 5:418–425. doi:10.1038/ni1049

Brossard, C., M. Semichon, A. Trautmann, and G. Bismuth. 2003. CD5 inhibits signaling at the immunological synapse without impairing its formation. *J. Immunol.* 170:4623–4629.

Budd, R.C., J.C. Cerottini, C. Horvath, C. Bron, T. Pedrazzini, R.C. Howe, and H.R. MacDonald. 1987. Distinction of virgin and memory T lymphocytes. Stable acquisition of the Pgp-1 glycoprotein concomitant with antigenic stimulation. *J. Immunol.* 138:3120–3129.

Croft, M., and C. Dubey. 1997. Accessory molecule and costimulation requirements for CD4 T cell response. *Crit. Rev. Immunol.* 17:89–118.

Dalloul, A. 2009. CD5: A safeguard against autoimmunity and a shield for cancer cells. *Auto. Rev.* 8:349–353. doi:10.1016/j.autrev.2008.11.007

Ernst, B., D.-S. Lee, J.M. Chang, J. Sprent, and C.D. Surh. 1999. The peptide ligands mediating positive selection in the thymus control T cell survival and homeostatic proliferation in the periphery. *Immunity.* 11:173–181. doi:10.1016/S1074-7613(00)80092-8

Eyrich, M., T. Croner, C. Leiler, P. Lang, P. Bader, T. Klingebiel, D. Niethammer, and P.G. Schlegel. 2002. Distinct contributions of CD4(+) and CD8(+) naive and memory T-cell subsets to overall T-cell-receptor repertoire complexity following transplantation of T-cell-depleted CD34-selected hematopoietic progenitor cells from unrelated donors. *Blood.* 100:1915–1918. doi:10.1182/blood-2001-11-0005

Fontenot, J.D., and A.Y. Rudensky. 2005. A well adapted regulatory contrivance: regulatory T cell development and the forkhead family transcription factor Foxp3. *Nat. Immunol.* 6:331–337. doi:10.1038/ni1179

Fontenot, J.D., M.A. Gavin, and A.Y. Rudensky. 2003. Foxp3 programs the development and function of CD4+CD25+ regulatory T cells. *Nat. Immunol.* 4:330–336. doi:10.1038/ni904

Freitas, A.A., and B.B. Rocha. 1993. Lymphocyte lifespans: homeostasis, selection and competition. *Immunol. Today.* 14:25–29. doi:10.1016/0167-5699(93)90320-K

Freitas, A.A., and B. Rocha. 2000. Population biology of lymphocytes: the flight for survival. *Annu. Rev. Immunol.* 18:83–111. doi:10.1146/annurev.immunol.18.1.83

Friedlein, G., F. El Hage, I. Vergnon, C. Richon, P. Saulnier, Y. Lécluse, A. Caignard, L. Boumsell, G. Bismuth, S. Chouaib, and F. Mami-Chouaib. 2007. Human CD5 protects circulating tumor antigen-specific CTL from tumor-mediated activation-induced cell death. *J. Immunol.* 178:6821–6827.

Ge, Q., H. Hu, H.N. Eisen, and J. Chen. 2002. Different contributions of thymopoiesis and homeostasis-driven proliferation to the reconstitution of naive and memory T cell compartments. *Proc. Natl. Acad. Sci. USA.* 99:2989–2994. doi:10.1073/pnas.052714099

Goldrath, A.W., and M.J. Bevan. 1999. Low-affinity ligands for the TCR drive proliferation of mature CD8+ T cells in lymphopenic hosts. *Immunity.* 11:183–190. doi:10.1016/S1074-7613(00)80093-X

Goldrath, A.W., L.Y. Bogatzki, and M.J. Bevan. 2000. Naive T cells transiently acquire a memory-like phenotype during homeostasis-driven proliferation. *J. Exp. Med.* 192:557–564. doi:10.1084/jem.192.4.557

Gorochov, G., A.U. Neumann, A. Kereveur, C. Parizot, T.S. Li, C. Katlama, M. Karmochkine, G. Raguin, B. Autran, and P. Debré. 1998. Perturbation of CD4+ and CD8+ T-cell repertoires during progression to AIDS and regulation of the CD4+ repertoire during antiviral therapy. *Nat. Med.* 4:215–221. doi:10.1038/nm0298-215

Greenberg, P.D., and S.R. Riddell. 1999. Deficient cellular immunity—finding and fixing the defects. *Science.* 285:546–551. doi:10.1126/science.285.5427.546

Han, M., L. Harrison, P. Kehn, K. Stevenson, J. Currier, and M.A. Robinson. 1999. Invariant or highly conserved TCR alpha are expressed on double-negative (CD3+CD4-CD8-) and CD8+ T cells. *J. Immunol.* 163:301–311.

Haribhai, D., W. Lin, B. Edwards, J. Ziegelbauer, N.H. Salzman, M.R. Carlson, S.H. Li, P.M. Simpson, T.A. Chatila, and C.B. Williams. 2009. A central role for induced regulatory T cells in tolerance induction in experimental colitis. *J. Immunol.* 182:3461–3468. doi:10.4049/jimmunol.0802535

Jameson, S.C. 2002. Maintaining the norm: T-cell homeostasis. *Nat. Rev. Immunol.* 2:547–556.

Jonsson, R., K.A. Brokstad, T. Hansen, T. Davies, and E. Ulvestad. 2002. The evolution and breakdown of the immune system: implications for development of autoimmune diseases. *Scand. J. Immunol.* 56:323–326. doi:10.1046/j.1365-3083.2002.01158.x

Jores, R., and T. Meo. 1993. Few V gene segments dominate the T cell receptor beta-chain repertoire of the human thymus. *J. Immunol.* 151:6110–6122.

Jorgensen, J.L., U. Esser, B. Fazekas de St Groth, P.A. Reay, and M.M. Davis. 1992. Mapping T-cell receptor-peptide contacts by variant

peptide immunization of single-chain transgenics. *Nature*. 355:224–230. doi:10.1038/355224a0

Kassiotis, G., R. Zamoyska, and B. Stockinger. 2003. Involvement of avidity for major histocompatibility complex in homeostasis of naive and memory T cells. *J. Exp. Med*. 197:1007–1016. doi:10.1084/jem.20021812

Khattri, R., T. Cox, S.A. Yasayko, and F. Ramsdell. 2003. An essential role for Scurfin in CD4+CD25+ T regulatory cells. *Nat. Immunol*. 4:337–342. doi:10.1038/ni909

Kimmig, S., G.K. Przybylski, C.A. Schmidt, K. Laurisch, B. Möwes, A. Radbruch, and A. Thiel. 2002. Two subsets of naive T helper cells with distinct T cell receptor excision circle content in human adult peripheral blood. *J. Exp. Med*. 195:789–794. doi:10.1084/jem.20011756

Kirberg, J., N. Bosco, J.-C. Deloulme, R. Ceredig, and F. Agenès. 2008. Peripheral T lymphocytes recirculating back into the thymus can mediate thymocyte positive selection. *J. Immunol*. 181:1207–1214.

Kretschmer, K., I. Apostolou, D. Hawiger, K. Khazaie, M.C. Nussenzweig, and H. von Boehmer. 2005. Inducing and expanding regulatory T cell populations by foreign antigen. *Nat. Immunol*. 6:1219–1227. doi:10.1038/ni1265

Lainscak, M., G.S. Filippatos, M. Gheorghiade, G.C. Fonarow, and S.D. Anker. 2008. Cachexia: common, deadly, with an urgent need for precise definition and new therapies. *Am. J. Cardiol*. 101:8E–10E. doi:10.1016/j.amjcard.2008.02.065

Lee, W.T., X.M. Yin, and E.S. Vitetta. 1990. Functional and ontogenetic analysis of murine CD45Rhi and CD45Rlo CD4+ T cells. *J. Immunol*. 144:3288–3295.

Lyons, A.B., and C.R. Parish. 1994. Determination of lymphocyte division by flow cytometry. *J. Immunol. Methods*. 171:131–137. doi:10.1016/0022-1759(94)90236-4

Maraskovsky, E., M. Teepe, P.J. Morrissey, S. Braddy, R.E. Miller, D.H. Lynch, and J.J. Peschon. 1996. Impaired survival and proliferation in IL-7 receptor-deficient peripheral T cells. *J. Immunol*. 157:5315–5323.

McMichael, A.J., and S.L. Rowland-Jones. 2001. Cellular immune responses to HIV. *Nature*. 410:980–987. doi:10.1038/35073658

Miller, R.A., C. Chrisp, and A. Galecki. 1997. CD4 memory T cell levels predict life span in genetically heterogeneous mice. *FASEB J*. 11:775–783.

Min, B., H. Yamane, J. Hu-Li, and W.E. Paul. 2005. Spontaneous and homeostatic proliferation of CD4 T cells are regulated by different mechanisms. *J. Immunol*. 174:6039–6044.

Moses, C.T., K.M. Thorstenson, S.C. Jameson, and A. Khoruts. 2003. Competition for self ligands restrains homeostatic proliferation of naive CD4 T cells. *Proc. Natl. Acad. Sci. USA*. 100:1185–1190. doi:10.1073/pnas.0334572100

Mucida, D., N. Kutchukhidze, A. Erazo, M. Russo, J.J. Lafaille, and M.A. Curotto de Lafaille. 2005. Oral tolerance in the absence of naturally occurring Tregs. *J. Clin. Invest*. 115:1923–1933. doi:10.1172/JCI24487

Mueller, D.L., S. Seiffert, W. Fang, and T.W. Behrens. 1996. Differential regulation of bcl-2 and bcl-x by CD3, CD28, and the IL-2 receptor in cloned CD4+ helper T cells. A model for the long-term survival of memory cells. *J. Immunol*. 156:1764–1771.

Pannetier, C. 1993. The sizes of the CDR3 hypervariable regions of the murine T cell receptor beta chains vary as a function of the recombined germ-line segments. *Proc. Natl. Acad. Sci. USA*. 90:4319–4323. doi:10.1073/pnas.90.9.4319

Pannetier, C., J. Even, and P. Kourilsky. 1995. T-cell repertoire diversity and clonal expansions in normal and clinical samples. *Immunol. Today*. 16:176–181. doi:10.1016/0167-5699(95)80117-0

Park, J.-H., Q. Yu, B. Erman, J.S. Appelbaum, D. Montoya-Durango, H.L. Grimes, and A. Singer. 2004. Suppression of IL7Ralpha transcription by IL-7 and other prosurvival cytokines: a novel mechanism for maximizing IL-7-dependent T cell survival. *Immunity*. 21:289–302. doi:10.1016/j.immuni.2004.07.016

Strong, J., Q. Wang, and N. Killeen. 2001. Impaired survival of T helper cells in the absence of CD4. *Proc. Natl. Acad. Sci. USA*. 98:2566–2571. doi:10.1073/pnas.051329698

Sudo, T., S. Nishikawa, N. Ohno, N. Akiyama, M. Tamakoshi, H. Yoshida, and S. Nishikawa. 1993. Expression and function of the interleukin 7 receptor in murine lymphocytes. *Proc. Natl. Acad. Sci. USA*. 90:9125–9129. doi:10.1073/pnas.90.19.9125

Surh, C.D., B. Ernst, and J. Sprent. 1992. Growth of epithelial cells in the thymic medulla is under the control of mature T cells. *J. Exp. Med*. 176:611–616. doi:10.1084/jem.176.2.611

Swain, S.L. 1994. Generation and in vivo persistence of polarized Th1 and Th2 memory cells. *Immunity*. 1:543–552. doi:10.1016/1074-7613(94)90044-2

Tan, J.T., E. Dudl, E. LeRoy, R. Murray, J. Sprent, K.I. Weinberg, and C.D. Surh. 2001. IL-7 is critical for homeostatic proliferation and survival of naive T cells. *Proc. Natl. Acad. Sci. USA*. 98:8732–8737. doi:10.1073/pnas.161126098

Viret, C., F.S. Wong, and C.A. Janeway Jr. 1999. Designing and maintaining the mature TCR repertoire: the continuum of self-peptide: self-MHC complex recognition. *Immunity*. 10:559–568. doi:10.1016/S1074-7613(00)80055-2

Wang, Z., C. Zhao, R. Moya, and J.D. Davies. 2008. A novel role for CD4+ T cells in the control of cachexia. *J. Immunol*. 181:4676–4684.

Williams, M.A., E.V. Ravkov, and M.J. Bevan. 2008. Rapid culling of the CD4+ T cell repertoire in the transition from effector to memory. *Immunity*. 28:533–545. doi:10.1016/j.immuni.2008.02.014

Wu, Z., S.J. Bensinger, J. Zhang, C. Chen, X. Yuan, X. Huang, J.F. Markmann, A. Kassaee, B.R. Rosengard, W.W. Hancock, et al. 2004. Homeostatic proliferation is a barrier to transplantation tolerance. *Nat. Med*. 10:87–92. doi:10.1038/nm965

Zhao, C., Z. Wang, M.W. Robertson, and J.D. Davies. 2008. Cachexia in the non-obese diabetic mouse is associated with CD4+ T-cell lymphopenia. *Immunology*. 125:48–58. doi:10.1111/j.1365-2567.2008.02819.x